PHILOSOPHICAL TRANSACTIONS — OF — **THE ROYAL SOCIETY** A | MATHEMATICAL, PHYSICAL & ENGINEERING SCIENCES

Two-parameter study of square-wave switching dynamics in orthogonally delay-coupled semiconductor lasers

C. Masoller, M. Sciamanna and A. Gavrielides

References	**This article cites 19 articles** http://rsta.royalsocietypublishing.org/content/371/1999/201204 71.full.html#ref-list-1
Subject collections	Articles on similar topics can be found in the following collections applied mathematics (110 articles) complexity (68 articles) optics (35 articles)
Email alerting service	Receive free email alerts when new articles cite this article - sign up in the box at the top right-hand corner of the article or click **here**

Research

CrossMark
click for updates

One contribution of 15 to a Theme Issue 'Dynamics, control and information in delay-coupled systems'.

Author for correspondence:
C. Masoller
e-mail: cristina.masoller@upc.edu

Two-parameter study of square-wave switching dynamics in orthogonally delay-coupled semiconductor lasers

C. Masoller[1], M. Sciamanna[2] and A. Gavrielides[3]

[1]Departament de Fisica i Enginyeria Nuclear, Universitat Politecnica de Catalunya, Colom 11, 08222 Terrassa, Barcelona, Spain
[2]Optics and Electronics (OPTEL) Research Group, Laboratoire Matériaux Optiques, Photonique et Systemes (LMOPS), Supélec, 2 Rue Edouard Belin, 57070 Metz, France
[3]Air Force Research Laboratory, AFR/EOARD, 86 Blenheim Crescent, Ruislip HA4 7HB, UK

We perform a detailed numerical analysis of square-wave (SW) polarization switching in two semi-conductor lasers with time-delayed, orthogonal mutual coupling. An in-depth mapping of the dynamics in the two-parameter plane coupling strength versus frequency detuning shows that stable SWs occur in narrow parameter regions that are localized close to the boundary of stability of the pure-mode solution. In this steady state, the two coupled lasers emit orthogonal polarizations. We also show that there are various types of SW forms and that stable switching does not need the inclusion of noise or nonlinear gain in the model. As these narrow regions of deterministic and stable SWs occur for quite different combinations of parameters, they could potentially explain the waveforms that have been observed experimentally. However, on the other hand, these regions are narrow enough to be in fact considered as experimentally unreachable. Therefore, our results indicate that further experimental statistical studies are needed in order to distinguish deterministic and stationary square waveforms from long transients because of noise.

1. Introduction

Recent years have seen an increased interest in understanding the physics and bifurcations at the origin

Royal Society **Publishing**
Informing the science of the future

of self-pulsating dynamics in a laser diode with time-delayed optical feedback or coupling. The increase in the feedback/coupling strength typically destabilizes the otherwise steady dynamics to self-pulsation with a period either close to the laser relaxation oscillation frequency or to the feedback/coupling delay time [1]. The waveform can vary from sharp pulsing to harmonic to square wave (SW) depending on the system nonlinearity [2–5], on the sub- or super-critical nature of the underlying Hopf bifurcation [5,6], on the laser mode competition or on the coupling/feedback parameters [7–15]. An interesting combination of these parameters is found in a recent experiment, where two edge-emitting laser diodes are mutually coupled through their orthogonal polarization modes [16]. Depending on the coupling strength and delay and on the mode competition (gain/loss ratio), the laser dynamics shows square waveforms with different time period and duty cycle. The dynamics has been reproduced numerically by a two-mode rate equation model with time-delayed coupling, including gain saturation and frequency detuning [17]. Although the dynamics was initially thought to be driven by noise, the numerical study has shown that square waveforms can be observed also in the deterministic model. The bifurcation at the origin of the SW dynamics has been very recently elucidated owing to advanced continuation techniques [18]. The bifurcation study has confirmed the deterministic scenario leading to SW dynamics: square waveforms result from a cascade of Hopf bifurcations on a two-mode steady state and become stable only in a narrow interval of the coupling strength close to a transcritical bifurcation to a one-mode steady-state solution. Previous works however have raised additional questions, e.g. how do the results depend on the model additional parameters such as gain saturation and detuning, and can we find a larger region of parameters where to observe stable SW dynamics?

We address here these pending issues on a system made of two laser diodes with delayed coupling of their orthogonal polarization modes. We complement our earlier numerical and bifurcation studies by an in-depth analysis of the dynamics in the two-parameter plane coupling strength versus frequency detuning and for different values of the gain saturation coefficients. We find several interesting new conclusions: (i) stable SWs always occur in narrow ranges of the coupling strength and detuning parameters close to the transition to the one-mode (pure mode, PM) steady state, but we find many such intervals of stable SWs in the whole parameter space, (ii) stable SWs can be observed also when the gain saturation coefficients are equal to zero, although in that case the SW dynamics acquire a fast weakly damped oscillation at the relaxation frequency of the laser in addition to the fundamental modulation at the coupling delay time and (iii) noise-free simulations show regions of parameters with stable SWs that are otherwise suppressed when including noise, hence suggesting coexistence of several other attractors. Our work brings therefore new light into the parameters leading to SW switching dynamics and motivates additional bifurcation studies in the two-parameter plane coupling strength versus frequency detuning.

Our paper is organized as follows. Section 2 details the rate equation model and parameters, as well as the steady states and their stability. Our numerical results on the mapping of the dynamics in the two-parameter plane are shown in §3. Our main conclusions are summarized in §4.

2. Model

(a) Model equations

The rate equations describing two identical semiconductor lasers mutually coupled through polarization-rotated optical injection are

$$\frac{\mathrm{d}E_{x,i}}{\mathrm{d}t} = k(1 + j\alpha)(g_{x,i} - 1)E_{x,i} + \sqrt{\beta_{\mathrm{sp}}}\xi_{x,i}, \tag{2.1}$$

$$\frac{\mathrm{d}E_{y,i}}{\mathrm{d}t} = j\delta E_{y,i} + k(1 + j\alpha)(g_{y,i} - 1 - \beta)E_{y,i} \tag{2.2}$$

$$+ \eta E_{x,3-i}(t - \tau) + \sqrt{\beta_{sp}} \xi_{y,i} \tag{2.3}$$

and
$$\frac{dN_i}{dt} = \gamma_N [\mu - N_i - g_{x,i} I_{x,i} - g_{y,i} I_{y,i}]. \tag{2.4}$$

Here, $i = 1$ and $i = 2$ denote the two lasers, E_x and E_y are orthogonal linearly polarized slowly varying complex amplitudes and N is the carrier density. In the absence of optical coupling the emission frequency of the two lasers is the same and is the frequency of the x-polarization that is taken as reference frequency, with δ being the angular frequency detuning between the x- and y-polarizations. The modal gains are

$$g_{x,i} = \frac{N_i}{(1 + \epsilon_{xx} I_{x,i} + \epsilon_{xy} I_{y,i})} \tag{2.5}$$

and

$$g_{y,i} = \frac{N_i}{(1 + \epsilon_{yx} I_{x,i} + \epsilon_{yy} I_{y,i})}. \tag{2.6}$$

Other parameters are k is the field decay rate, γ_N is the carrier decay rate, α is the linewidth enhancement factor, β is the linear loss anisotropy, β_{sp} is the noise strength, $\xi_{x,y}$ are uncorrelated Gaussian white noises and μ is the injection current parameter, normalized such that the solitary threshold is at $\mu_{th} = 1$. The parameters of the polarization-orthogonal mutual coupling are η and τ, which represent the coupling strength and the delay time, respectively.

(b) Steady-state solutions

The model has two types of steady states. The first is the mixed-mode (MM) solution, in which the two coupled lasers emit the x- and y-polarizations simultaneously, with

$$I_{1x} = I_{2x} = I_x, \tag{2.7}$$

$$I_{1y} = I_{2y} = I_y \tag{2.8}$$

and
$$N_1 = N_2 = N. \tag{2.9}$$

I_x, I_y and N can be calculated from the following coupled set of equations for I_x, I_y and g_y:

$$\mu - 1 - (1 + \epsilon_{xx}) I_x - \epsilon_{xy} I_y - g_y I_y = 0, \tag{2.10}$$

$$g_y = \frac{1 + \epsilon_{xx} I_x + \epsilon_{xy} I_y}{1 + \epsilon_{yx} I_x + \epsilon_{yy} I_y} \tag{2.11}$$

and
$$\eta^2 = \frac{I_y}{I_x} ([\delta + k\alpha(g_y - 1 - \beta)]^2 + k^2(g_y - 1 - \beta)^2). \tag{2.12}$$

Equation (2.10) results from setting the time derivative of the carried density equal to zero, and eliminating N with $N = 1 + \epsilon_{xx} I_x + \epsilon_{xy} I_y$ (that results from $g_x = 1$). Equation (2.11) is obtained from equations (2.5) and (2.6) using $g_x = 1$ and $N_1 = N_2 = N$. Equation (2.12) results from solving the field rate equations taking into account that the frequency of the y-polarization locks to the frequency of the injected x-polarization.

The procedure to solve these equations is as follows. Given $I_y > 0$, I_x is calculated from equation (2.10): by substituting g_y using equation (2.11), $I_x > 0$ is a solution of a second-order polynomial on I_y. With I_x and I_y, then g_y is calculated from equation (2.11), the coupling strength, η, from equation (2.12), and the carrier density from $N = 1 + \epsilon_{xx} I_x + \epsilon_{xy} I_y$.

The second type of steady state is the PM solution, in which one laser emits the x-polarization while the other laser emits the y-polarization. The coupling between the lasers in this solution is unidirectional, the laser that emits the x-polarization acts as 'master' laser, and the laser that emits the y-polarization acts as 'injected' laser.

For the master (solitary) laser, the trivial steady state is

$$I_x = \frac{\mu - 1}{1 + \epsilon_{xx}} \tag{2.13}$$

and

$$N_x = 1 + \epsilon_{xx} I_x. \tag{2.14}$$

For the injected laser, the intensity and carrier density, I_y and N_y, can be calculated from two coupled equations for I_y and g_y,

$$\mu - g_y(1 + \epsilon_{yy} I_y) - g_y I_y = 0 \tag{2.15}$$

and

$$\eta^2 = \frac{I_y}{I_x}([\delta + k\alpha(g_y - 1 - \beta)]^2 + k^2(g_y - 1 - \beta)^2). \tag{2.16}$$

These equations are obtained in the same way as for the MM solution (i.e. by setting the time derivative of the carrier density equal to zero, and by solving the field rate equations taking into account that the frequency of the y-polarization locks to the frequency of the injected x-polarization). In equation (2.15), we used

$$g_y = \frac{N_y}{1 + \epsilon_{yy} I_y} \tag{2.17}$$

to eliminate N_y.

The procedure to solve the coupled equations is the same as that described for the MM solution: given $I_y > 0$ we compute g_y from equation (2.15). With g_y and I_x (calculated from equation (2.13)), we obtain the coupling strength from equation (2.16) and the carrier density from equation (2.17).

For typical parameter values, with $I_x, I_y > 0$ there is only one MM solution, and either one or three PM solutions, depending on the coupling strength.

(c) Stability of the steady states

The stability of the PM and MM solutions was analysed in [17,18], and here we present a brief summary of the main results.

As the PM solution corresponds to a unidirectional coupling situation, in which there is no back delayed coupling from the injected laser to the master laser, its stability depends on the coupling strength, η, but does not depend on the delay time of the coupling, τ. For increasing η, the PM undergoes a bifurcation that is of transcritical type due to a change of sign of a real eigenvalue [18]. The bifurcation occurs at a value of the coupling strength, η_c, that can be calculated from equation (2.16) with I_x and g_y calculated from equations (2.13) and (2.17), respectively, and $I_y > 0$ being a solution of the polynomial equation

$$\epsilon_{xy}(1 + \epsilon_{yy})I_y^2 + [1 - (\mu - 1)\epsilon_{yy} + \epsilon_{xy}]I_y - (\mu - 1) = 0. \tag{2.18}$$

In addition, the PM solution can undergo a Hopf bifurcation that brings time-dependent solutions with a frequency close to the laser relaxation oscillation.

The MM becomes unstable after a supercritical Hopf bifurcation, after which symmetric $(I_{1x} = I_{2x}, I_{1y} = I_{2y}, N_1 = N_2)$ time-dependent solutions emerge, with a frequency also close to the relaxation oscillation. At higher coupling strengths, several Hopf bifurcations of the now unstable mixed state occur. These bifurcations give rise to time-periodic solutions that are initially unstable, but they can become stable at larger coupling strengths, in narrow intervals of the coupling η. The periodicity of these initially unstable solutions grows with the coupling and, at large η, unstable SW solutions emerge from Hopf bifurcations of the unstable mixed state, that have a periodicity close to the delay τ or close to 2τ. These solutions can later become stable, at higher values of η, in narrow intervals of η values.

The analysis done by Sciamanna *et al.* [18] (by using continuation methods, and also numerically, by simulating the model equations) demonstrated that these SW solutions do not need and are not supported by the addition of noise, but are stable only in narrow parameter regions. By contrast, in the analysis by Sukow *et al.* [16], using a simpler model (without gain saturation and without frequency detuning) only transient SW dynamics were found. An interesting issue that remains to be investigated is to what extent the stability of SW dynamics depends on these parameters, and if there is any role of the noise. In the next section we address these issues by presenting the results of extended numerical simulations of the model equations, displaying different types of SW switching dynamics.

3. Numerical results

The simulation of the model equations was carried out considering the same parameters as in the earlier studies [17,18], unless otherwise explicitly indicated: $k = 300\,\mathrm{ns}^{-1}$, $\mu = 2$, $\alpha = 3$, $\gamma_N = 0.5\,\mathrm{ns}^{-1}$, $\beta = 0.04$, $\epsilon_{xx} = 0.01$, $\epsilon_{xy} = 0.015$, $\epsilon_{yx} = 0.02$, $\epsilon_{yy} = 0.025$, $\beta_{\mathrm{sp}} = 10^{-5}\,\mathrm{ns}^{-1}$, $\tau = 3\,\mathrm{ns}$. For these parameters, without coupling the lasers emit the x-polarization. The angular frequency detuning between the two polarizations, δ, and the coupling strength, η, will be considered as control parameters.

### (a) Stable square-wave switching in the parameter space (η, δ)

For each set of parameters (η, δ), we integrated a trajectory, starting from initial conditions with both lasers off, until a stable output was reached (and the trajectory approached one of the model fixed points), or the maximum integration time was reached, $6\,\mu\mathrm{s}$. Figure 1*a* presents in grey scale the stationary state of the coupled lasers as a function of η and δ. MM or PM indicates mixed-mode or pure-mode steady state, respectively; PO or IO indicates periodic or irregular oscillations respectively; and SW indicates regular square-wave switching.

The lifetime of the transient dynamics is plotted in grey scale in figure 1*b* and is defined as the time interval during which the amplitude of the fluctuations of the intensity of the x-polarization of both lasers, measured in terms of the standard deviation calculated in a time window, is above a certain value (4% of the average intensity). In other words, we considered that the transient dynamics finished when the fluctuations of either I_{1x} or I_{2x} are below the threshold; if at the end of the simulation the dynamics of the coupled lasers is such that both I_{1x} and I_{2x} are still time-dependent, with oscillations larger than the threshold, then the duration of the transient is considered to be equal to the integration time ($6\,\mu\mathrm{s}$).

Although the MM solution is usually reached very fast, the transient towards the PM solution tends to be much longer and depends on the noise level, as will be discussed later. In figure 1*a*, regular SWs (black dots) occur in several very narrow parameter regions that are located very close to the boundary of stability of the PM solution (in figure 1*a* the black line indicates the solution of equation (2.18), i.e. the location of the transcritical bifurcation in the parameter plane (η, δ)). Much longer simulations with parameters chosen in these narrow windows reveal that the SWs are indeed stable. A few examples of the waveforms are displayed in figure 2 that plots the time traces of the intensities, I_x and I_y, of one of the lasers (the corresponding parameters are indicated with triangles in figure 1).

Many black dots, which are randomly scattered within the region of stability of the PM (top-right corner in figure 1*a*), represent also regular SWs; however, in this parameter region longer simulations reveal that the SWs are a transient dynamics that eventually finishes when the PM is found.

While in the study of Masoller *et al.* [17] stable SWs were found only in a narrow range of negative detuning values, in figure 1*a* we can observe that they also occur at certain positive values of δ. In the various narrow regions of SW switching, the shape of the SWs can change considerably, as shown in figure 2. This suggests that the SWs in different regions might originate from different sequences of bifurcations of the MM solution.
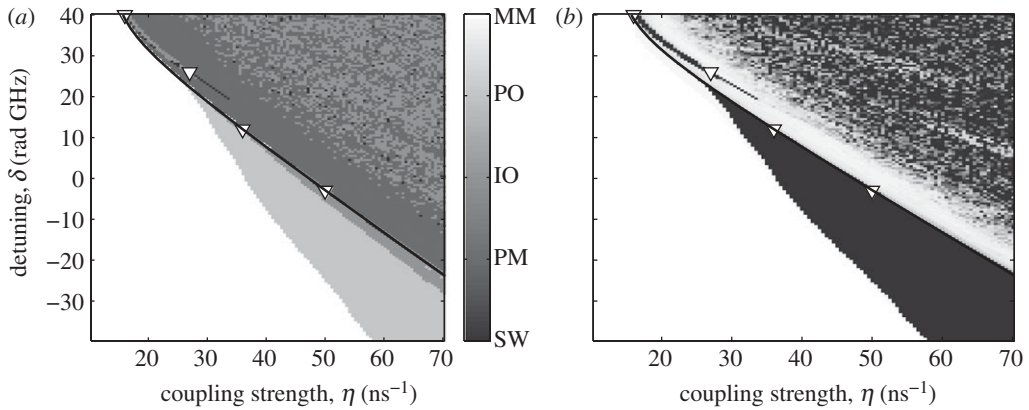
Figure 1. (a) Phase diagram in the parameter space (coupling strength, detuning). The grey colour scale indicates the stationary behaviour, from white to black: mixed-mode solution (MM), periodic oscillations (PO), irregular oscillations (IO), pure-mode solution (PM) and square-wave switching (SW). The black line displays the solution of equation (2.18) and the triangles indicate the parameters of figure 2a–d. (b) Duration of the transient time, in grey scale (white, a few tens of ns; black, 6 µs). The parameters are as indicated in the text.
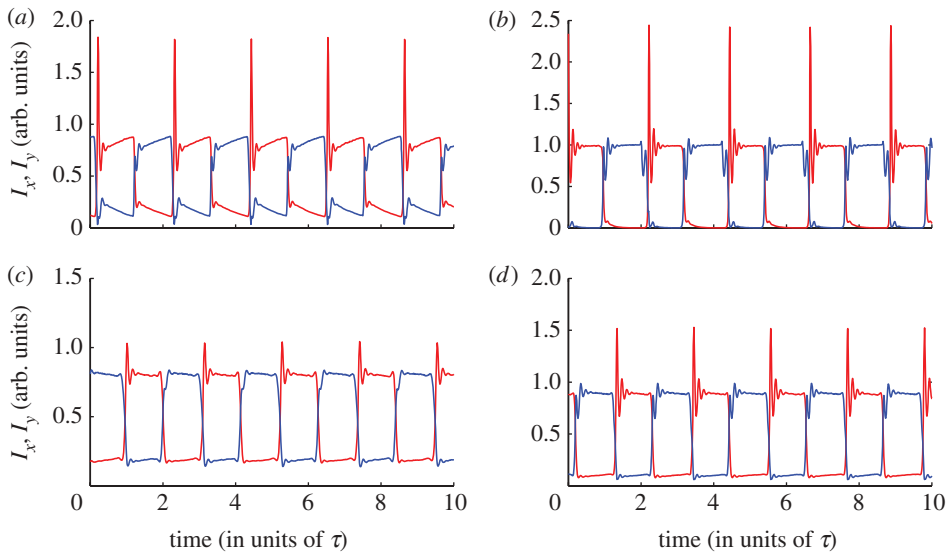

Figure 2. Stable SW solutions. The x and y intensities of one laser are plotted versus time. The x intensity (red in the online version) displays sharp spikes when it turns on, while the y intensity (blue in the online version) turns on without spikes. The parameters are (indicated with triangles in figure 1): (a) $\eta = 16\,\text{ns}^{-1}$, $\delta = 40\,\text{rad GHz}$; (b) $\eta = 27\,\text{ns}^{-1}$, $\delta = 26\,\text{rad GHz}$; (c) $\eta = 36\,\text{ns}^{-1}$, $\delta = 12\,\text{rad GHz}$; (d) $\eta = 50\,\text{ns}^{-1}$, $\delta = -3\,\text{rad GHz}$. (Online version in colour.)

Outside the narrow windows of stable switching and near the boundary of stability of the PM solution, the stationary dynamics, after a long SW switching transient, tends to the emission of pulses with orthogonal polarizations: one laser emits the x-polarization and with certain periodicity emits one or more pulses in the y-polarization; while the other laser emits the y-polarization and, also with the same periodicity, emits one or more pulses in the x-polarization.

(b) Influence of gain saturation and noise

In the study of Masoller *et al.* [17], the SWs were found for a specific set of the gain saturation coefficients (such that $\epsilon_{xx} < \epsilon_{xy} < \epsilon_{yx} < \epsilon_{yy}$). Here, we have done a detailed analysis of the
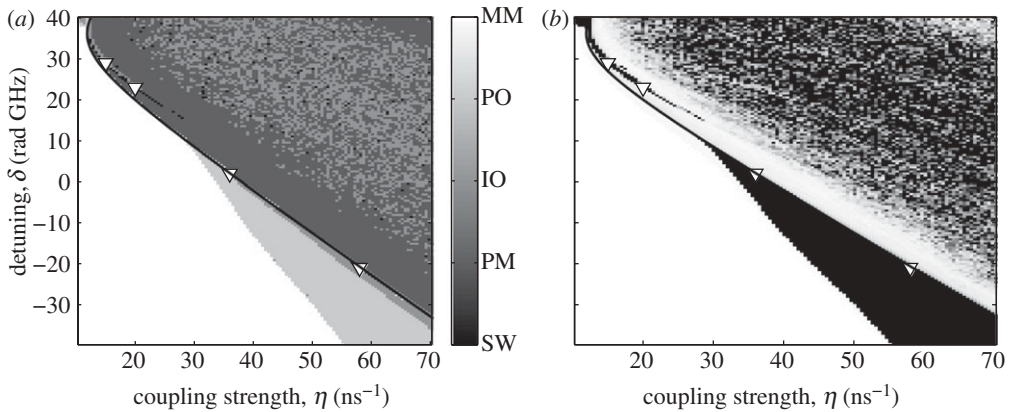
Figure 3. Stationary dynamics in the parameter space (coupling strength, angular frequency detuning) (*a*) and duration of the transient time (*b*). The grey scale is the same as in figure 1, the black line displays the solution of equation (2.18), and the triangles indicate the parameters of figure 4*a*–*d*. The gain saturation coefficients are all equal ($\epsilon_{xx} = \epsilon_{xy} = \epsilon_{yx} = \epsilon_{yy} = 0.01$), and other parameters are as indicated in the text.
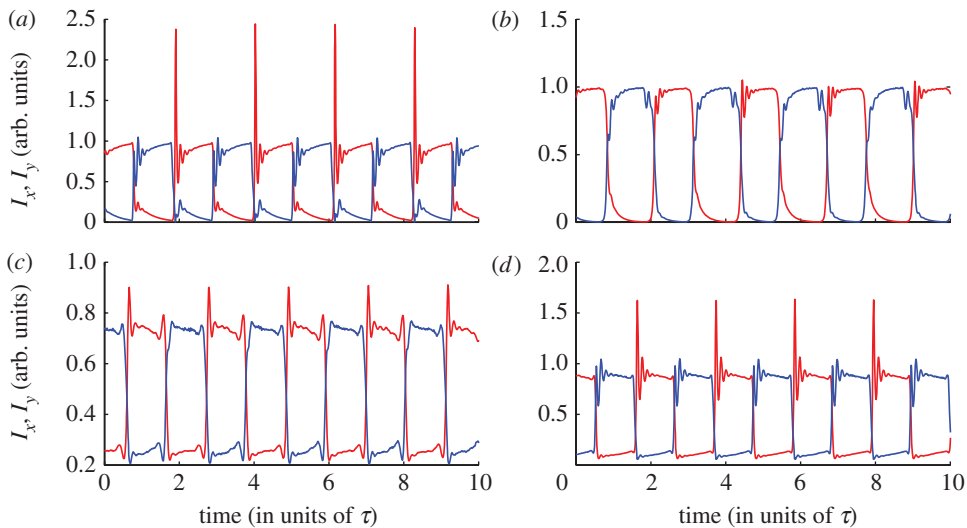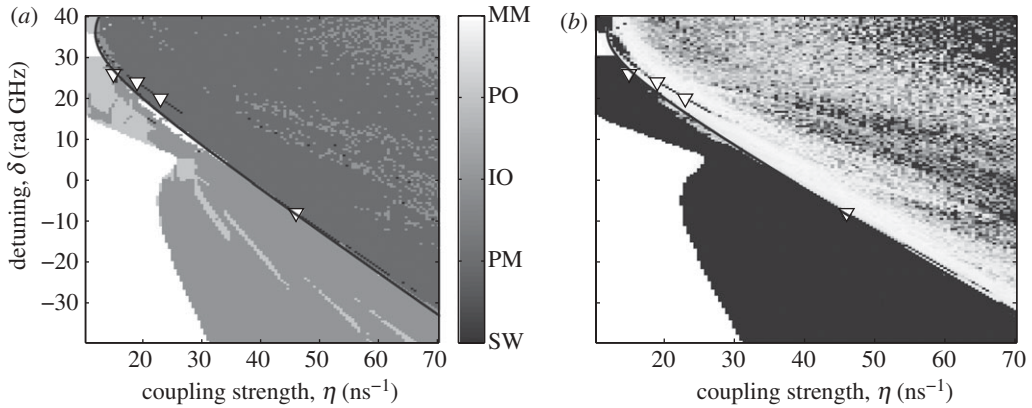

Figure 4. SW switching when the gain saturation coefficients are all equal to 0.01. The coupling and detuning parameters are (indicated with triangles in figure 3): (*a*) $\eta = 15\,\text{ns}^{-1}$, $\delta = 29\,\text{rad GHz}$; (*b*) $\eta = 21\,\text{ns}^{-1}$, $\delta = 22\,\text{rad GHz}$; (*c*) $\eta = 36\,\text{ns}^{-1}$, $\delta = 2\,\text{rad GHz}$; (*d*) $\eta = 58\,\text{ns}^{-1}$, $\delta = -21\,\text{rad GHz}$. (Online version in colour.)

parameter space (δ, η) varying also the gain saturation coefficients and found that stable SWs occur indeed in narrow regions but for many combinations of the gain saturation coefficients, including when they are all equal, as shown in figures 3 and 4. In fact, we found that in order to observe stable SWs, there is no need to include gain saturation in the model, and these are seen in narrow regions, also with $\epsilon_{xx} = \epsilon_{xy} = \epsilon_{yx} = \epsilon_{yy} = 0$ (figure 5); however, without gain saturation the SWs display more undamped fast pulsations at the relaxation oscillation frequency. A few examples of waveforms are displayed in figure 6.

The waveform in figure 6*a*, for fixed detuning $\delta = 26\,\text{rad GHz}$ is stable in the range of coupling strengths $14.5\,\text{ns}^{-1} < \eta < 15.5\,\text{ns}^{-1}$. In this range, the waveform maintains the quasi-periodic structure of fast relaxation oscillations modulated by the slower coupling delay time. This waveform is found below the boundary of instability of the PM solution (at $\eta = 15.5\,\text{ns}^{-1}$ for $\delta = 26\,\text{rad GHz}$) and we did not find coexistence of the two solutions.

Figure 5. As figures 1 and 3 but without gain saturation ($\epsilon_{xx} = \epsilon_{xy} = \epsilon_{yx} = \epsilon_{yy} = 0$). The black line displays the solution of equation (2.18) and the triangles indicate the parameters of figure 6a–d.
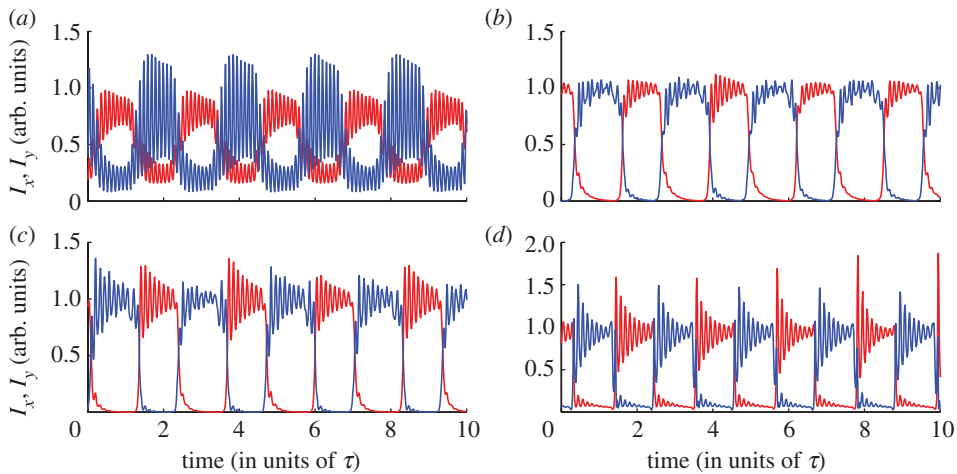

Figure 6. SW-like switching when in the simulations the gain saturation coefficients are set equal to 0. The coupling and detuning parameters are (indicated with triangles in figure 5): (a) $\eta = 15 \, \text{ns}^{-1}$, $\delta = 26 \, \text{rad GHz}$; (b) $\eta = 19 \, \text{ns}^{-1}$, $\delta = 24 \, \text{rad GHz}$; (c) $\eta = 23 \, \text{ns}^{-1}$, $\delta = 20 \, \text{rad GHz}$; (d) $\eta = 46 \, \text{ns}^{-1}$, $\delta = -8 \, \text{rad GHz}$. (Online version in colour.)

The waveforms displayed in figure 6b,c are stable within a range of (η, δ) values that is wider than the typical intervals where stable SWs are found. In spite of the fact that this range of values is embedded in the region of stability of the PM solution, we could not find, trying with different initial conditions, any coexistence of stable SWs and the PM solution.

The waveform displayed in figure 6d is stable in the small range $45.76 \, \text{ns}^{-1} < \eta < 46.15 \, \text{ns}^{-1}$ for $\delta = -8 \, \text{rad GHz}$ and coexists with similar other waveforms that can be captured by using different initial conditions. For $\eta > 46.15 \, \text{ns}^{-1}$, the SWs decay to the PM after long transients.

Thus, to summarize, the above-presented results demonstrate that, although the intervals of coupling strengths where there are stable SWs are usually narrow, they occur for quite different combinations of parameters, and thus we can expect that their existence explains the measurements in the earlier studies [16,17], and confirms the stability of the experimentally observed SW forms.

However, an important issue in the stability of the numerical solutions is the role of noise. The results of deterministic simulations (setting $\beta_{\text{sp}} = 0$), presented in figures 7 and 8 for the same parameters as figures 1 and 5, respectively, demonstrate that the narrow regions of stable SWs
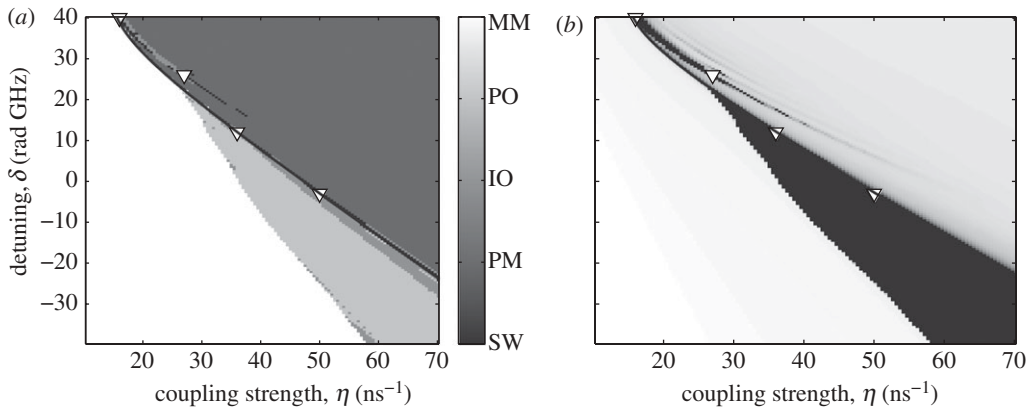
Figure 7. As figure 1 but with no noise included in the simulations. The black line displays the solution of equation (2.18) and the triangles indicate the parameters of figure 2a–d.
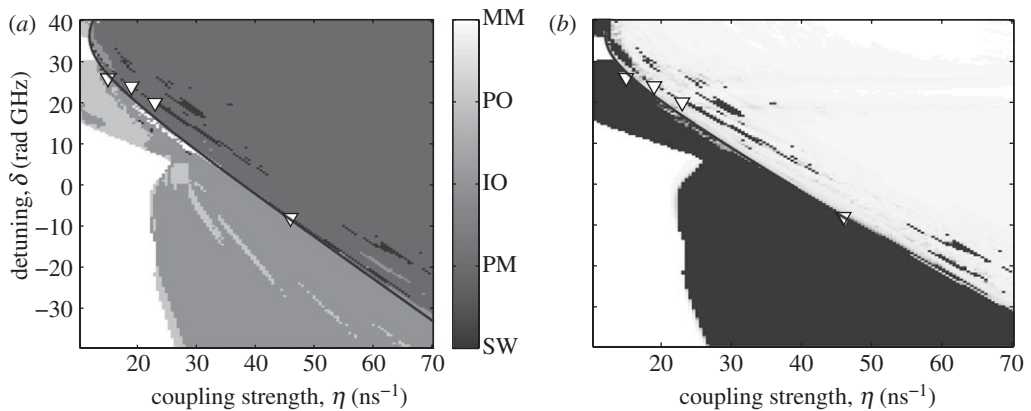
Figure 8. As figure 5 but with no noise included in the simulations. The black line displays the solution of equation (2.18) and the triangles indicate the parameters of figure 6a–d.

persist. As expected from the analysis by Sciamanna *et al.* [18], the stable SWs are not supported and do not need the addition of noise. One can also note, by comparing figures 7b and 8b with figures 1b and 5b that the duration of the transient dynamics towards the PM solution is significantly shorter in the absence of noise, whereas the duration of the transient towards the MM is almost unaffected.

As the transient dynamics towards the PM consists of SW switchings that gradually become irregular, it is also possible that the SWs observed experimentally in the earlier studies [16,17] are in fact a transient induced by the presence of noise. 'Deterministic' stable SW switching occurs in such narrow parameter regions that in fact these regions can be considered as experimentally unreachable.

It is also worth noting that a comparison of figure 7 with figure 1 reveals that in the absence of noise, no additional regions of stable SWs are seen; i.e. the simulations without noise presented in figure 7 do not reveal SWs that were not already found in the stochastic simulations presented in figure 1. On the contrary, when the simulations are done with $\epsilon_{xx} = \epsilon_{xy} = \epsilon_{yx} = \epsilon_{yy} = 0$, as seen in figure 8, the noise-free simulations reveal several new regions of stable SWs, when compared with those in figure 5. These regions are located inside the region where the PM solution is stable. Deterministic simulations starting with different initial conditions reveal that these waveforms are indeed stable; however, in the stochastic simulations, small fluctuations allow the trajectory

to eventually find the coexisting stable PM solution. Thus, while for most parameters within the region of stable PM the inclusion of noise results in long, SW switching transients (when compared with deterministic simulations), for certain parameters, noise has the opposite effect. In noiseless simulations, there is stable SW switching while in stochastic simulations, the switching is a transient and the trajectory eventually finds the PM (that is not found in the absence of noise).

4. Conclusions

To conclude, we performed a detailed analysis of SW polarization switching in two semiconductor lasers with time-delayed, orthogonal mutual coupling. We found that the general behaviour of the system is as follows: for low enough coupling the MM fixed point is stable (in this state, the two lasers emit the two polarizations simultaneously); whereas for high enough coupling the PM fixed point is stable (in this state the two lasers emit orthogonal polarizations). In between these two regions, there are time-dependent solutions that arise from bifurcations of the PM or of the MM. Stable SW switching was found in very narrow parameter regions that were located near the boundary of stability of the PM solution. In these narrow regions, we found different types of SW forms and carefully checked their stability. Our results show that, in the simpler model without nonlinear gain, stable SWs also occur in narrow parameter regions, and exhibit a fast weakly damped oscillation at the relaxation frequency of the laser in addition to the fundamental modulation at the coupling delay time. Finally, we studied the influence of noise and showed that it usually (but not always) enlarges the duration of the SW switching transient when compared with deterministic simulations.

We found numerically that there are many parameter intervals where there are stable SWs, and these intervals occur for quite different combinations of parameters. Thus, we could speculate that our results explain the SW forms experimentally measured in [16,17] or confirm their stability. However, since noise induces long, SW transient dynamics towards the PM, it is also possible that the waveforms observed experimentally were in fact noise-induced, because the 'deterministic' and stable SWs (that do not need the inclusion of noise) occur in such narrow parameter regions that in fact these regions could be considered as experimentally unreachable. Thus, we hope that our results will motivate new experimental studies with focus on the statistical properties of the switchings, that would allow clarification of this issue, if they are a deterministic or a noise-sustained dynamics.

For future work, to shed light onto this issue, it would be interesting to analyse the polarization switching dynamics using nonlinear methods of time-series analysis, such as ordinal analysis [19, 20]. Varying the laser pump current (a parameter that can be easily controlled experimentally) would allow exploration of the parameter region close to the laser threshold, where a stronger influence of noise could be expected, when compared with the region that has been studied so far, which is above twice the threshold [16–18].

References

1. Kane DM, Shore KA. 2005 *Unlocking dynamical diversity: optical feedback effects on semiconductor lasers*. New York, NY: Wiley.
2. Larger L, Goedgebuer J-P, Merolla J-M. 1998 Chaotic oscillator in wavelength: a new setup for investigating differential difference equations describing nonlinear dynamics. *IEEE J. Quantum Electron.* **34**, 594–601. (doi:10.1109/3.663432)

3. Erneux T, Larger L, Lee MW, Goedgebuer J-P. 2004 Ikeda Hopf bifurcation revisited. *Physica D* **194**, 49–64. (doi:10.1016/j.physd.2004.01.038)

4. Chembo Kouomou Y, Colet P, Larger L, Gastaud N. 2005 Chaotic breathers in delayed electro-optical systems. *Phys. Rev. Lett.* **95**, 203903. (doi:10.1103/PhysRevLett.95.203903)

5. Sciamanna M, Mégret P, Blondel M. 2004 Hopf bifurcation cascade in small-α laser diodes subject to optical feedback. *Phys. Rev. E* **69**, 046209. (doi:10.1103/PhysRevE.69.046209)

6. Larger L, Goedgebuer J-P, Erneux T. 2004 Subcritical Hopf bifurcation in dynamical systems described by a scalar nonlinear delay differential equation. *Phys. Rev. E* **69**, 036210. (doi:10.1103/PhysRevE.69.036210)

7. Jiang S, Pan Z, Dagenais M, Morgan RA, Kojima K. 1993 High-frequency polarization self-modulation in vertical-cavity surface emitting lasers. *Appl. Phys. Lett.* **63**, 3545–3547. (doi:10.1063/1.110092)

8. Robert F, Besnard P, Charès ML, Stéphan G. 1997 Polarization modulation dynamics of vertical-cavity surface-emitting lasers with an extended cavity. *IEEE J. Quantum Electron.* **33**, 2231–2239. (doi:10.1109/3.644106)

9. Li H, Hohl A, Gavrielides A, Hou H, Choquette KD. 1998 Stable polarization self-modulation in vertical-cavity surface-emitting lasers. *Appl. Phys. Lett.* **72**, 2355–2357. (doi:10.1063/1.121398)

10. Sciamanna M, Erneux T, Rogister F, Deparis O, Mégret P, Blondel M. 2002 Bifurcation bridges between external-cavity modes lead to polarization self-modulation in vertical-cavity surface-emitting lasers. *Phys. Rev. A* **65**, 041801(R). (doi:10.1103/PhysRevA.65.041801)

11. Sciamanna M, Rogister F, Deparis O, Mégret P, Blondel M, Erneux T. 2002 Bifurcation to polarization self-modulation in vertical-cavity surface-emitting lasers. *Opt. Lett.* **27**, 261–263. (doi:10.1364/OL.27.000261)

12. Heil T, Uchida A, Davis P, Aida T. 2003 TE-TM dynamics in a semiconductor laser subject to polarization-rotated optical feedback. *Phys. Rev. A* **68**, 033811. (doi:10.1103/PhysRevA.68.033811)

13. Gavrielides A, Erneux T, Sukow DW, Burner G, McLachlan T, Miller J, Amonette J. 2006 Square-wave self-modulation in diode lasers with polarization-rotated optical feedback. *Opt. Lett.* **31**, 2006–2008. (doi:10.1364/OL.31.002006)

14. Gavrielides A, Sukow DW, Burner G, McLachlan T, Miller J, Amonette J. 2010 Simple and complex square waves in an edge-emitting diode laser with polarization-rotated optical feedback. *Phys. Rev. E* **81**, 056209. (doi:10.1103/PhysRevE.81.056209)

15. Mashal L, Van der Sande G, Gelens L, Danckaert J, Verschaffelt G. 2012 Square-wave oscillations in semiconductor ring lasers with delayed optical feedback. *Opt. Express.* **20**, 22503–22516. (doi:10.1364/OE.20.022503)

16. Sukow DW, Gavrielides A, Erneux T, Mooneyham B, Lee L, McKay J, Davis J. 2010 Asymmetric square waves in mutually coupled semiconductor lasers with orthogonal optical injection. *Phys. Rev. E* **81**, 025206(R). (doi:10.1103/PhysRevE.81.025206)

17. Masoller C, Sukow DW, Gavrielides A, Sciamanna M. 2011 Bifurcation to square-wave switching in orthogonally delay-coupled semiconductor lasers: theory and experiment. *Phys. Rev. A* **84**, 023838. (doi:10.1103/PhysRevA.84.023838)

18. Sciamanna M, Virte M, Masoller C, Gavrielides A. 2012 Hopf bifurcation to square-wave switching in mutually coupled semiconductor lasers. *Phys. Rev. E* **86**, 016218. (doi:10.1103/PhysRevE.86.016218)

19. Masoller C, Rosso OA. 2011 Quantifying the complexity of the delayed logistic map. *Phil. Trans. R. Soc. A* **369**, 425–438. (doi:10.1098/rsta.2010.0281)

20. Rubido N, Tiana-Alsina J, Torrent MC, Garcia-Ojalvo J, Masoller C. 2011 Language organization and temporal correlations in the spiking activity of an excitable laser: experiments and model comparison. *Phys. Rev. E* **84**, 026202. (doi:10.1103/PhysRevE.84.026202)